Published in final edited form as:
In Vitro Cell Dev Biol Anim. 2007 ; 43(3-4): 139–146. doi:10.1007/s11626-007-9016-6.

UXT (Ubiquitously Expressed Transcript) causes mitochondrial aggregation

Tijuana N. Moss, **Amy Vo**, **Wallace L. McKeehan**, and **Leyuan Liu**
Center for Cancer and Stem Cell Biology, Institute of Biosciences and Technology, Texas A&M Health Science Center, Texas Medical Center, 2121 W. Holcombe Boulevard, Houston, TX 77030, USA

Abstract

Mitochondria are the bioenergetic and metabolic centers in eukaryotic cells and play a central role in apoptosis. Mitochondrial distribution is controlled by the microtubular cytoskeleton. The perinuclear aggregation of mitochondria is one of the characteristics associated with some types of cell death. Control of mitochondrial aggregation particularly related to cell death events is poorly understood. Previously, we identified ubiquitously expressed transcript (UXT) as a potential component of mitochondrial associated LRPPRC, a multidomain organizer that potentially integrates mitochondria and the microtubular cytoskeleton with chromosome remodeling. Here we show that when overexpressed in mammalian cells, green fluorescent protein-tagged UXT (GFP-UXT) exhibits four types of distribution patterns that are proportional to the protein level, and increase with time. UXT initially was dispersed in the extranuclear cytosol, then appeared in punctate cytosolic dots, then an intense perinuclear aggregation that eventually invaded and disrupted the nucleus. The punctate cytosolic aggregates of GFP-UXT coincided with aggregates of mitochondria and LRPPRC. We conclude that increasing concentrations of UXT contributes to progressive aggregation of mitochondria and cell death potentially through association of UXT with LRPPRC.

Keywords

Apoptosis; Cell death; C19ORF5; LRPPRC; RASSF1A; Prefoldin; Microtubule-associated proteins

Introduction

The human gene for ubiquitously expressed transcript (UXT) is located in the Xp11.23-p11.22 region containing several different disease loci (Schroer et al. 1999; Thiselton et al. 2002). The gene of generally unknown function comprised of seven exons encoding a protein of 157 amino acids was named because of the wide expression and high conservation in the mouse (Schroer et al. 1999; Liu and McKeehan 2002; Markus et al. 2002). Reports concerning the relative expression level between normal and tumor tissues have been conflicting. The abundant expression in tumor tissues such as bladder, breast, ovary, and thyroid and the induction of cell death by siRNA knockdown suggested a positive role in tumor promotion through enhancement of cell viability (Zhao et al. 2005). In contrast, a reported decreased expression in prostate cancer tissue concurrent with an

lliu@ibt.tamhsc.edu .
Present address: T. N. Moss, BioVeris Corporation, 16020 Industrial Drive, Lab 1-146, Gaithersburg, MD 20877-1414, USA

inhibition of cell growth by overexpression suggested a role in growth suppression (Taneja et al. 2004). Conflicting results have been published within the same research group (Markus et al. 2002; Taneja et al. 2004).

To decipher the function of UXT, several groups have attempted to identify its interactive patterns. UXT was first found to interact with mitochondria-associated leucine-rich pentatricopeptide repeat motif-containing (LRPPRC) protein (Liu and McKeehan 2002), mitotic checkpoint protein BUB3 and CBP/p300-interactive transcriptional factor CITED2 (Liu et al. 2002). Subsequently, UXT, renamed as ART-27, was reported to interact with the androgen receptor, and a role in male sex determination, prostate development and malignant growth was proposed (Markus et al. 2002). UXT was also found to interact with a calcineurin-bound Down's syndrome candidate region 1 (DSCR1) protein that is overexpressed in Down's syndrome patients (Silveira et al. 2004), and centrosome-associated protein phosphatase Cdc14A (Zhao et al. 2005).

LRPPRC is a mitochondria-associated protein (Liu et al. 2002; Mili and Pinol-Roma 2003; Mootha et al. 2003), and a mutant of it is associated with Leigh Syndrome, a French-Canadian type (LSFC), a cytochrome *c* oxidase deficiency disease (Mootha et al. 2003). In addition to UXT, LRPPRC also interacts with microtubule-associated protein homologue, C19ORF5 (Liu et al. 2002; Liu and McKeehan 2002). C19ORF5 associates with hyperstabilized microtubules, causes mitochondria aggregation and genome destruction at elevated level (Liu et al. 2005a), and binds with mitochondria-associated paclitaxel-like microtubular stabilizer RASSF1A and potentially mediates RASSF1A tumor suppression (Liu et al. 2005b). Unlike C19ORF5, UXT does not associate with microtubules under conditions tested thus far (Liu et al. 2002; Moss, Liu and McKeehan, unpublished results). These observations and the dependence of mitochondrial distribution and function on the microtubular cytoskeleton (Desagher and Martinou 2000; Kroemer et al. 1998) prompted us to reexamine the potential impact of UXT on mitochondria and coincidental cell functions.

Here we show that when overexpressed in mammalian cells, UXT exhibits four types of distribution patterns proportional to the protein level that progressively increased with time. At low protein levels, UXT is mainly distributed in the extranuclear cytosol and gradually forms perinuclear aggregates overlapping with aggregated mitochondria as protein level increases. The aggregates finally invade and destroy the nucleus. The interaction of UXT with LRPPRC discovered by yeast two-hybrid screening was confirmed in a mammalian cell context. UXT colocalized with LRPPRC and the aggregated mitochondria. We propose that UXT may contribute to mitochondrial aggregation and cell death possibly through its interaction with LRPPRC.

Materials and Methods

Expression of GFP- and Hemagglutinin (HA)-tagged UXT in COS7 cells

The GFP-UXT construct was reconstructed from a previously reported construct (Liu et al. 2002) by ligating the end-filled 0.5 kb *Eco*RI-*Xho*I cut fragment from UXT-pACT2 with the end-filled *Hin*dIII cut pEGFP-C3 vector (Clontech, Mountain View, CA) as described (Liu et al. 2002). Additionally, a HA-UXT construct was created by ligation of end-filled 0.5 kb *Eco*RI-*Bam*HI cut fragment from UXT-pGBKT7 (Liu et al. 2002) with end-filled *Sal*I cut pCMV-HA vector (Clontech). Both constructs were validated by DNA sequencing and expression products described in the text. COS7 cells were cultured and transiently transfected as described (Liu et al. 2002). The expressed products were confirmed by immunoblotting using antibody against GFP, HA, and UXT (1B2, a gift from Dr. Qiang Wang, University of Pennsylvania) as described (Liu et al. 2005a).

Fixation, immunofluorescence, microscopy, and image capture

The transfected COS7 cells were processed for direct fluorescence analysis, mitochondria labeling using MitoTracker® Red CM-H2XRos (MitoTracker), or further immunostaining of LRPPRC using monoclonal antibody 9C9 (a gift from Dr. Serafín Pińol-Roma, Mount Sinai School of Medicine, New York) as described (Liu et al. 2002). Cells on coverslips were washed once with 1 X PBS and counterstained with 4 μg/ml of 4,6-diamidino-2-phenylindole (DAPI, Sigma-Aldrich) for 1 min where needed. The coverslips were mounted and sealed in Aqua Poly/Mount (Polysciences, Inc., Warrington, PA) for microscopic analysis. All images were captured using a CoolSNAP *ES* Monochrome camera from Photometrics®, Roper Scientific (Tucson, AZ) through an Olympus 1X70 inverted scope using an X40/1.35 oil iris (Olympus America Life Science Resources, Ltd., Melville, NY) under the control of MetaVue program (Downingtown, PA).

Coimmunoprecipitation of HA-UXT with endogenous LRPPRC or BUB3

About 1×10^6 COS7 cells in a 75 cm^2 flask were transiently transfected with about 12 μg of HA-UXT or pCMV-HA vector and lysed in 250 μl of immunoprecipitation (IP) buffer containing 50 mM Hepes (pH 7.5), 150 mM NaCl, 5 mM EDTA, 1 mM phenylmethanesulfonyl (PMSF), 10 μg/ml aprotonin, 1 mM NaF, 10% glycerol, and 0.1% Triton X-100. The same 9 μg of HA antibody and 50 μl of packed volume of protein G-agarose beads were incubated with each sample containing 200 μl cell lysate for 30 min. One-fourth of the precipitate resuspended in 100 μl immuno-precipitation (IP) buffer (corresponding to 2.5×10^5 cells) was subjected to immunoblot with 0.1 μg/ml antibody against HA, LRPPRC, or BUB3 (BL1686, Santa Cruz Biotechnology, Santa Cruz, CA). The proteins were visualized using alkaline phosphate-conjugated antibodies.

Results

Time-dependent appearance of transfected UXT in perinuclear aggregates

We first determined the impact and time-dependent subcellular localization of UXT in COS7 cells transfected with UXT with a GFP tag at the N-terminus. Cells transiently transfected with a similar efficiency of 30% exhibited a similar level of both GFP-UXT and a GFP control (Fig. 1*a*). Beginning at 10.5 h post transfection, we observed a progressive perinuclear aggregation of the GFP signal that was generally classified into four different stages (types I–IV cell morphologies) (Fig. 1*b*). The fluorescence intensities from type I to type IV cells are markedly increased and the differences were detectable by our naked eyes. We have reported the increases in both the maximal fluorescence intensities (about 15 fold) and the protein level (about five fold) of GFP-C19ORF5 from type I to type IV cells (Liu et al. 2005a). In this aspect, UXT is very similar to C19ORF5 based on our observation. However, images shown here and in figures below were taken with optional exposure times to achieve the best resolution. The actual intensities for type III to type IV are much higher than the shown. Type I and type II cells appeared to represent the majority of cells at the earliest stage when display of GFP-UXT was lowest. The type I distribution was characterized by dot-like structures smoothly dispersed in the entire cytosol. This is in contrast to a previously reported result which showed distribution of the GFP signal presumably reporting distribution of UXT in both cytosol and nucleus (Liu et al. 2002). The GFP-UXT construct was subsequently shown to contain a sequencing error within coding sequence for UXT downstream of GFP. An authentic GFP-UXT product is mainly distributed in the cytosol (Fig. 1). Type II cells were similar to the type I distribution except that punctate foci in dot-like structures were apparent scattered among the general cytosolic distribution of the signal. A minor portion of the transfected cells classified as a type III distribution exhibited a dramatic perinuclear aggregation of the GFP-UXT that was increased in fluorescence intensity. An even more intense aggregation occurred in small

number of type IV cells where GFP-UXT aggregates formed ball-like structures that eventually engulfed the entire nuclei. Unlike the type I–type III cells that exhibited intact nuclei, the nucleus was disintegrated with clearly a diminished DNA content in type IV cells. When expressed unattached to UXT, the GFP protein dispersed uniformly in both nuclei and cytosol both in apparently healthy cells (Fig. 1*c*, top panel) and in classic apoptotic cells with condensed nuclei in which DNA was still largely intact (Fig. 1*c*, bottom panel). The characteristic perinuclear aggregation observed with GFP-UXT was not detectable in cells transfected with GFP alone. We conclude that it is the UXT portion of GFP-UXT that caused the specific distribution patterns of GFP-UXT.

Time-dependent perinuclear aggregation of UXT and cell death

To determine whether the perinuclear condensation of GFP-UXT was progressive and whether the type III and type IV phenotypes arose from type I and type II cells, cells of all four morphologies were counted directly. The number of type III and type IV cells increased linearly with time over a 48-h period (Fig. 2*a*). At 48 h the combined number of cells was three times that observed at 10.5 h. After 48 h type IV cells (Fig. 1) exhibiting a disintegrating nucleus and nuclear GFP-UXT detached from the culture surface and disintegrated. This was in contrast to the constant number of conventional apoptotic cells (30–40%; Fig. 2*b*) in cells expressing only GFP.

Perinuclear aggregates of UXT colocalize with perinuclear aggregates of mitochondria

The perinuclear aggregates of GFP-UXT in type III cells were suggestive of mitochondrial aggregates that have been observed in cells overexpressing another LRPPRC-interactive protein, C19ORF5 (Liu et al. 2005a). To determine whether the perinuclear aggregates of GFP-UXT were colocalized with mitochondria, we labeled mitochondria in cells transfected with GFP-UXT using red MitoTracker, a dye that specifically concentrates in mitochondria by active import (Pendergrass et al. 2004). In normal type I cells in which GFP-UXT was disperse, mitochondria distributed in their characteristic punctate pattern similar to cells expressing GFP or untransfected cells (Fig. 3). Type II cells that begin to exhibit some GFP-UXT aggregation exhibited a proportional amount of apparent mitochondrial aggregation. The intensely yellow signal in type III and type IV cells that exhibited intensely red fused aggregates of mitochondria and aggregated foci of green UXT indicated that UXT and mitochondrial aggregates were essentially superimposed (Fig. 3).

UXT colocalizes with LRPPRC in the aggregated mitochondria

LRPPRC is a multicompartmental protein that appears in small quantities in the nucleus, the cytosol and is most prominently associated with the mitochondria where a mutant form is thought to impact mitochondrial oxidative function (Liu et al. 2002; Mootha et al. 2003; Mili and Pinol-Roma 2003). Figure 4 shows that endogenous LRPPRC in red exhibits the normal punctate distribution associated with normal mitochondria in type I cells, whereas GFP-UXT is distributed smoothly in the cytosol. The increasing intensity of the yellow overlapping signal of red LRPPRC and green GFP-UXT indicated that LRPPRC tracks with the progressive aggregation of UXT and that both are presumably associated with the aggregating mitochondria (Fig. 3).

UXT interacts directly with LRPPRC and mitotic checkpoint protein BUB3

Yeast two-hybrid screening revealed that both LRPPRC, a mitochondria-associated protein, and BUB3, a protein involved in mitotic checkpoint mechanism, interact with UXT (Liu et al. 2002). To determine whether the interaction occurred in a mammalian cell context, we transfected UXT tagged with HA at the N-terminus into COS cells, captured the HA-UXT with HA antibody from the cell lysates and then subsequently analyzed immunoprecipitates

with antibodies against LRPPRC and BUB3 to probe for presence of cellular LRPPRC and BUB3. The results confirmed that both LRPPRC and BUB3 were present in the HA-UXT immunoprecipitates, but not in control precipitates from untransfected cells or cells transfected with the pCMV-HA vector devoid of UXT cDNA (Fig. 4).

We then determined whether LRPPRC and BUB3 colocalize with elevated levels of transfected GFP-UXT and the progressive transition of cells from type I to type IV caused by the transfection. LRPPRC protein progressively colocalized with the increasing aggregates of GFP-UXT and mitochondria observed in type III and type IV cells (Fig. 5). No overlap of GFP-UXT and endogenous BUB3 was observed (data not shown).

Discussion

Mitochondria are the bioenergetic and metabolic centers in eukaryotic cells and play a central role in cell life and death (Kroemer et al. 1998; Desagher and Martinou 2000). Aggregation and perinuclear clustering of mitochondria has been observed to be associated with some forms of cell death, although the role of mitochondrial aggregation as an active participant or consequential endpoint in each type remains to be established (De Vos et al. 1998; Desagher and Martinou 2000; Suen et al. 2000; Thomas et al. 2000). Diverse forms of perinuclear aggregation of mitochondria have been reported to be associated with activation of tumor necrosis factor (TNF) (De Vos et al. 1998; Suen et al. 2000; Thomas et al. 2000), treatment with staurosporine (Frank et al. 2001), expression of hepatitis B virus X protein (Takada et al. 1999), the Bcl-2-related pro-apoptotic protein Bax (Wolter et al. 1997; Desagher and Martinou 2000), Bim (Puthalakath et al. 1999), and Bid (Li et al. 1998). Through motor proteins as plus-end-directed kinesin and minus-end-directed dynein (Hirokawa 1998), microtubules act as the major component of cytoskeletal systems that underpin mitochondrial transport and homeostasis in mammalian cells (Heggeness et al. 1978). Microtubule stabilizer, paclitaxel, induced accumulation of mitochondria and mitochondrial DNA (mtDNA) replication (Karbowski et al. 2001). Microtubule-associated proteins such as MAP2, tau, and MAP4 generally stabilize MT tracks (Ebneth et al. 1998) or regulate the attachment or detachment of organelles to the tracks (Trinczek et al. 1999). KIF1B, an MT plus-end-directed monomeric motor protein for transport of mitochondria, is localized in mitochondria (Nangaku et al. 1994). Accordingly, disruption of the microtubule-associated protein tau (Sato et al. 2002) and motor protein kinesin (Desagher and Martinou 2000; Tanaka et al. 1998) causes perinuclear clustering of aggregated mitochondria.

In previous reports, we described the discovery and characterization of SEC1 domain interactive proteins of LRPPRC, a multidomain protein involved in mitochondrial trafficking controlled by the microtubular cytoskeleton (Liu et al. 2002; Liu and McKeehan 2002). The SEC1 domain interactive proteins of LRPPRC are C19ORF5, UXT, and CECR2. C19ORF5 is a sequence homologue of microtubule-associated proteins MAP1A and MAP1B, associates with hyperstabilized microtubules induced by specifically the A isoform of the putative tumor suppressor RASSF1, and at elevated concentrations promotes mitochondrial aggregation culminating with cell death (Liu et al. 2002, 2005a). We have proposed that these two activities may be linked to constitute a cell death mechanism triggered by prolonged hyperstabilization of microtubules during mitosis or in other cellular events.

In contrast, UXT exhibits no sequence homology to microtubule-associated proteins and no association with microtubules (Liu et al. 2002; Moss, Liu and McKeehan, unpublished results). UXT is a prefoldin-like protein and interacts with γ-tubulin (Zhao et al. 2005). Prefoldin acts as a post-chaperonin tubulin folding cofactor and regulates microtubule

dynamics (Lopez-Fanarraga et al. 2001). Tubulin is an inherent component of the voltage-dependent anion channel (VDAC) on mitochondrial membranes that controls the permeability transition pore (PTP) (Carre et al. 2002). Here we show that despite these differences, UXT at elevated concentrations causes mitochondrial aggregation and cell death similar to C19ORF5. The mitochondrial aggregation and cell death activities of C19ORF5 have been narrowed to a 25-amino acid sequence that is conserved among MAPs, but has no homology in UXT (Liu et al. 2005a). Thus, it remains to be determined whether UXT and C19ORF5 converge at a similar or different point to trigger mitochondrial aggregation. UXT also interacts with DSCR1, human Down's syndrome critical region gene 1 (Silveira et al. 2004). The *Drosophila melanogaster* homolog of DSCR1 is associated with mitochondria, and a regulator of mitochondrial function and integrity, and thus DSCR1 has been proposed to play a role in the mitochondrial dysfunction observed in Down's syndrome (Chang and Min 2005).

Lastly, the association of UXT with centrosomes under some conditions (Zhao et al. 2005) and its interaction with BUB3 is consistent with the proposed role of LRPPRC and its interactive proteins in monitoring spindle quality, fidelity of chromosome separation, and mitotic progression (Liu et al. 2002, 2005a, b). Although we failed to demonstrate colocalization of UXT and BUB3 in interphase cells, cell cycle synchronization experiments are in progress to determine if the interaction occurs during a specific window of the cell cycle.

Acknowledgments

This work was supported by Public Health Service Grants DK35310 from NIDDK, CA59971 and Minority Supplement Grant 3 R01 CA59971-14S from NCI, National Institutes of Health. We thank Dr. Qiang Wang, University of Pennsylvania, and Dr. Serafín Piñol-Roma of Mount Sinai School of Medicine (New York, New York) for mouse monoclonal antibody against UXT and LRPPRC, respectively, and Dr. Jian Kuang, Dept. of Cellular Oncology, MD Anderson Cancer Center for helpful advice.

References

Carre M, Andre N, Carles G, et al. Tubulin is an inherent component of mitochondrial membranes that interacts with the voltage-dependent anion channel. J. Biol. Chem. 2002; 277:33664–33669. [PubMed: 12087096]

Chang KT, Min KT. Drosophila melanogaster homolog of Down syndrome critical region 1 is critical for mitochondrial function. Nat. Neurosci. 2005; 8:1577–1585. [PubMed: 16222229]

De Vos K, Goossens V, Boone E, et al. The 55-kDa tumor necrosis factor receptor induces clustering of mitochondria through its membrane-proximal region. J. Biol. Chem. 1998; 273:9673–9680. [PubMed: 9545301]

Desagher S, Martinou JC. Mitochondria as the central control point of apoptosis. Trends Cell Biol. 2000; 10:369–377. [PubMed: 10932094]

Ebneth A, Godemann R, Stamer K, et al. Overexpression of tau protein inhibits kinesin-dependent trafficking of vesicles, mitochondria, and endoplasmic reticulum: implications for Alzheimer's disease. J. Cell Biol. 1998; 143:777–794. [PubMed: 9813097]

Frank S, Gaume B, Bergmann-Leitner ES, et al. The role of dynamin-related protein 1, a mediator of mitochondrial fission, in apoptosis. Dev. Cell. 2001; 1:515–525. [PubMed: 11703942]

Heggeness MH, Simon M, Singer SJ. Association of mitochondria with microtubules in cultured cells. Proc. Natl. Acad. Sci. U S A. 1978; 75:3863–3866. [PubMed: 80800]

Hirokawa N. Kinesin and dynein superfamily proteins and the mechanism of organelle transport. Science. 1998; 279:519–526. [PubMed: 9438838]

Karbowski M, Spodnik JH, Teranishi M, et al. Opposite effects of microtubule-stabilizing and microtubule-destabilizing drugs on biogenesis of mitochondria in mammalian cells. J. Cell Sci. 2001; 114:281–291. [PubMed: 11148130]

Kroemer G, Dallaporta B, Resche-Rigon M. The mitochondrial death/life regulator in apoptosis and necrosis. Annu. Rev. Physiol. 1998; 60:619–642. [PubMed: 9558479]

Li H, Zhu H, Xu CJ, Yuan J. Cleavage of BID by caspase 8 mediates the mitochondrial damage in the Fas pathway of apoptosis. Cell. 1998; 94:491–501. [PubMed: 9727492]

Liu L, McKeehan WL. Sequence analysis of LRPPRC and its SEC1 domain interaction partners suggest roles in cytoskeletal organization, vesicular trafficking, nucleocytosolic shuttling and chromosome activity. Genomics. 2002; 79:124–136. [PubMed: 11827465]

Liu L, Vo A, Liu G, McKeehan WL. Novel complex integrating mitochondria and the microtubular cytoskeleton with chromosome remodeling and tumor suppressor RASSF1 deduced by in silico homology analysis, interaction cloning in yeast, and colocalization in cultured cells. In Vitro Cell. Dev. Biol. Anim. 2002; 38:582–594. [PubMed: 12762840]

Liu L, Vo A, Liu G, McKeehan WL. Distinct structural domains within C19ORF5 support association with stabilized microtubules and mitochondrial aggregation and genome destruction. Cancer Res. 2005a; 65:4191–4201. [PubMed: 15899810]

Liu L, Vo A, McKeehan WL. Specificity of the methylation-suppressed A isoform of candidate tumor suppressor RASSF1 for microtubule hyperstabilization is determined by cell death inducer C19ORF5. Cancer Res. 2005b; 65:1830–1838. [PubMed: 15753381]

Lopez-Fanarraga M, Avila J, Guasch A, et al. Review: post-chaperonin tubulin folding cofactors and their role in microtubule dynamics. J. Struct. Biol. 2001; 135:219–229. [PubMed: 11580271]

Markus SM, Taneja SS, Logan SK, et al. Identification and characterization of ART-27, a novel coactivator for the androgen receptor N terminus. Mol. Biol. Cell. 2002; 13:670–682. [PubMed: 11854421]

Mili S, Pinol-Roma S. LRP130, a pentatricopeptide motif protein with a noncanonical RNA-binding domain, is bound in vivo to mitochondrial and nuclear RNAs. Mol. Cell Biol. 2003; 23:4972–4982. [PubMed: 12832482]

Mootha VK, Lepage P, Miller K, et al. Identification of a gene causing human cytochrome c oxidase deficiency by integrative genomics. Proc. Natl. Acad. Sci. U S A. 2003; 100:605–610. [PubMed: 12529507]

Nangaku M, Sato-Yoshitake R, Okada Y, et al. KIF1B, a novel microtubule plus end-directed monomeric motor protein for transport of mitochondria. Cell. 1994; 79:1209–1220. [PubMed: 7528108]

Pendergrass W, Wolf N, Poot M. Efficacy of MitoTracker Green and CMXrosamine to measure changes in mitochondrial membrane potentials in living cells and tissues. Cytometry A. 2004; 61:162–169. [PubMed: 15382028]

Puthalakath H, Huang DC, O'Reilly LA, et al. The proapoptotic activity of the Bcl-2 family member Bim is regulated by interaction with the dynein motor complex. Mol. Cell. 1999; 3:287–296. [PubMed: 10198631]

Sato S, Tatebayashi Y, Akagi T, et al. Aberrant tau phosphorylation by glycogen synthase kinase-3beta and JNK3 induces oligomeric tau fibrils in COS-7 cells. J. Biol. Chem. 2002; 277:42060–42065. [PubMed: 12191990]

Schroer A, Schneider S, Ropers H, Nothwang H. Cloning and characterization of UXT, a novel gene in human Xp11, which is widely and abundantly expressed in tumor tissue. Genomics. 1999; 56:340–343. [PubMed: 10087202]

Silveira HC, Sommer CA, Soares-Costa A, Henrique-Silva F. A calcineurin inhibitory protein overexpressed in Down's syndrome interacts with the product of a ubiquitously expressed transcript. Braz. J. Med. Biol. Res. 2004; 37:785–789. [PubMed: 15264020]

Suen YK, Fung KP, Choy YM, et al. Concanavalin A induced apoptosis in murine macrophage PU5-1.8 cells through clustering of mitochondria and release of cytochrome c. Apoptosis. 2000; 5:369–377. [PubMed: 11227218]

Takada S, Shirakata Y, Kaneniwa N, Koike K. Association of hepatitis B virus X protein with mitochondria causes mitochondrial aggregation at the nuclear periphery, leading to cell death. Oncogene. 1999; 18:6965–6973. [PubMed: 10597295]

Tanaka Y, Kanai Y, Okada Y, et al. Targeted disruption of mouse conventional kinesin heavy chain, kif5B, results in abnormal perinuclear clustering of mitochondria. Cell. 1998; 93:1147–1158. [PubMed: 9657148]

Taneja SS, Ha S, Swenson NK, et al. ART-27, an androgen receptor coactivator regulated in prostate development and cancer. J. Biol. Chem. 2004; 279:13944–13952. [PubMed: 14711828]

Thiselton DL, McDowall J, Brandau O, et al. An integrated, functionally annotated gene map of the DXS8026-ELK1 interval on human Xp11.3-Xp11.23: potential hotspot for neurogenetic disorders. Genomics. 2002; 79:560–572. [PubMed: 11944989]

Thomas WD, Zhang XD, Franco AV, et al. TNF-related apoptosis-inducing ligand-induced apoptosis of melanoma is associated with changes in mitochondrial membrane potential and perinuclear clustering of mitochondria. J. Immunol. 2000; 165:5612–5620. [PubMed: 11067917]

Trinczek B, Ebneth A, Mandelkow EM, Mandelkow E. Tau regulates the attachment/detachment but not the speed of motors in microtubule-dependent transport of single vesicles and organelles. J. Cell Sci. 1999; 112(Pt 14):2355–2367. [PubMed: 10381391]

Wolter KG, Hsu YT, Smith CL, et al. Movement of Bax from the cytosol to mitochondria during apoptosis. J. Cell Biol. 1997; 139:1281–1292. [PubMed: 9382873]

Zhao H, Wang Q, Zhang H, et al. UXT is a novel centrosomal protein essential for cell viability. Mol. Biol. Cell. 2005; 16:5857–5865. [PubMed: 16221885]

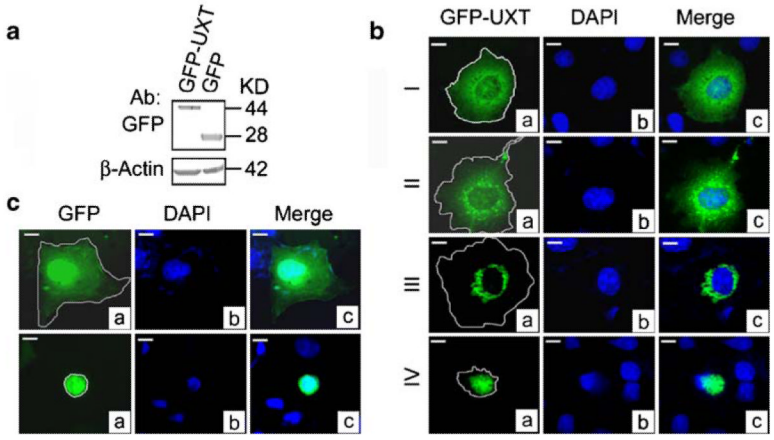

Figure 1.

Cellular distribution of GFP-UXT. (*a*) Immunoblot of GFP-UXT or GFP from extracts of transfected cells indicate intact expression products. (*b*) Four general morphologic profiles of GFP distribution in COS7 cells transfected with GFP-UXT. Cells were classified as type I to type IV based on increasing intensity of perinuclear aggregation. (*c*) Cells transfected with the GFP vector. General cytosolic and nuclear distribution expected of GFP in normal cells (*top panel*). Conventional apoptotic cells exhibiting a condensed, but intact nuclei and GFP within it. Cell boundaries were located by light microscope and traced as indicated. *Bar*, 10 μm in all photomicrographs.

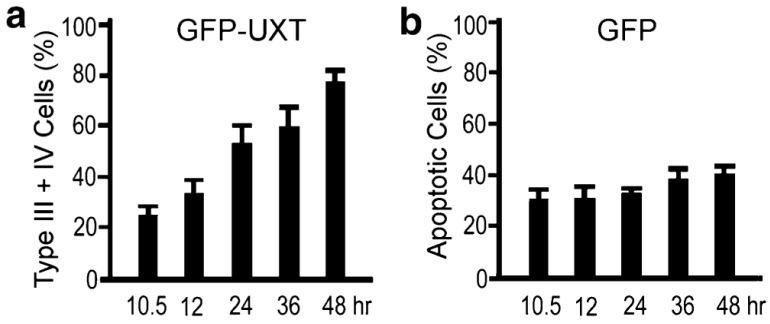

Figure 2.

(*a*) Time dependent increase of type III and type IV cells exhibiting perinuclear aggregation of GFP-UXT. (*b*) Conventional apoptotic cells as in Fig. 1*c* expressing GFP alone. Data are the mean+SD of three independent experiments in which least 1,000 transfected type III plus IV cells or apoptotic cells were counted.

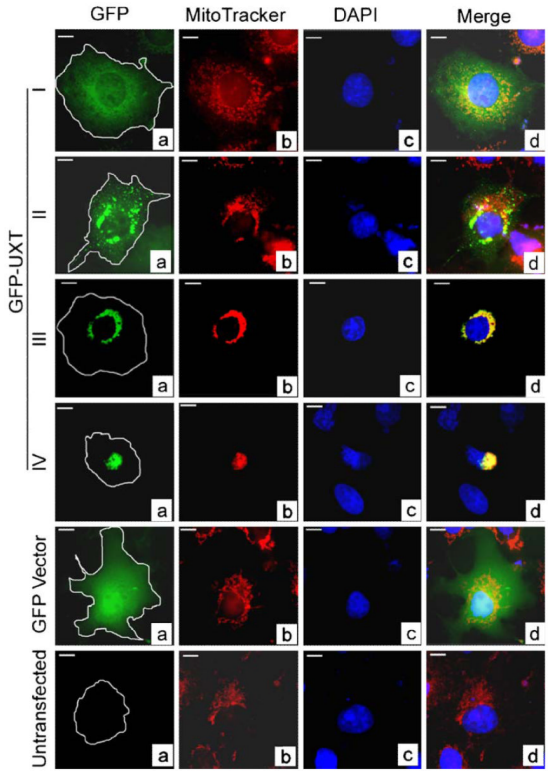

Figure 3.

Colocalization of aggregates of GFP-UXT and mitochondria. Green GFP (*a*), *red* MitoTracker-stained mitochondria (*b*), and *blue* DAPI-stained nuclei (*c*) were merged in (*d*). Yellow represents overlap of UXT with mitochondria and cyan overlap of GFP with nuclear DNA.

Figure 4.

Interaction of UXT with LRPPRC and BUB3 in mammalian cells. COS7 cells transfected with HA-UXT or only HA were lysed and subjected to immunoprecipitation with anti-HA monoclonal antibody immobilized on protein G sepharose beads. The precipitated complex was subjected to immunoblot analysis using antibodies against LRPPRC, BUB3, or HA as indicated on the *left*. The blots represent lysate from 5×10^3 cells. Untransfected cell lysates are also indicated. Total, whole-cell lysate; HAIP, immunoprecipitates with the HA antibody.

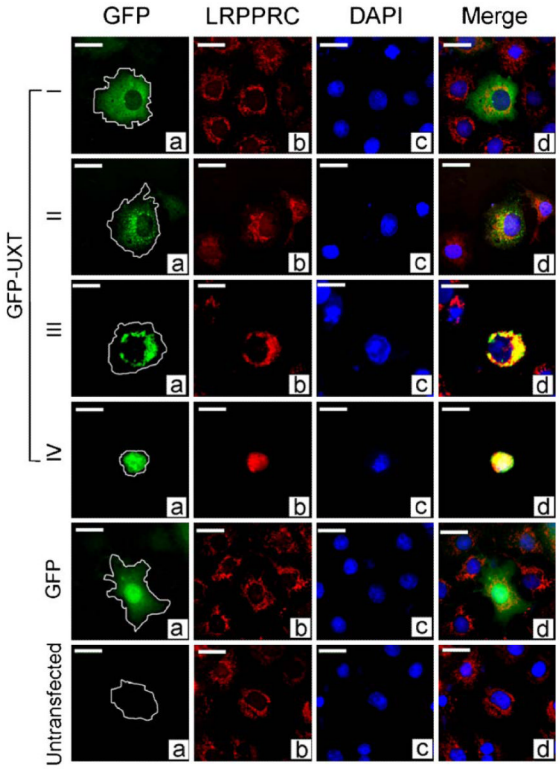

Figure 5.
Colocalization of UXT and LRPPRC. Cells transfected with GFP-UXT or GFP were analyzed with antibody against LRPPRC. Green GFP (*a*), red LRPPRC (*b*), and blue DAPI (DNA) (*c*) were merged in (*d*). Yellow indicates overlap of UXT and LRPPRC.